

Stable Transfection of Urokinase-Type Plasminogen Activator Antisense Construct Modulates Invasion of Human Glioblastoma Cells¹

Sanjeeva Mohanam, Sushma L. Jasti, Sudha R. Kondraganti, Nirmala Chandrasekar, Yoshiaki Kin, Gregory N. Fuller, Sajani S. Lakka, Athanassios P. Kyritsis, Dzung H. Dinh, William C. Olivero, Meena Gujrati, W. K. A. Yung, and Jasti S. Rao²

Division of Cancer Biology, Department of Biomedical and Therapeutic Sciences [S. M., N. C., S. S. L., J. S. R.] and Departments of Neurosurgery [D. H. D., W. C. O., J. S. R.] and Pathology [M. G.], University of Illinois College of Medicine at Peoria, Peoria, Illinois 61656, and Departments of Neurosurgery [S. R. K., Y. K.], Neuro-Oncology [S. L. J., A. P. K., W. K. A. Y.], and Neuropathology [G. N. F.], The University of Texas M. D. Anderson Cancer Center, Houston, Texas 77030

ABSTRACT

The diffuse and extensive infiltration of malignant gliomas into the surrounding normal brain is believed to rely on modifications of the proteolysis of extracellular matrix components. A key molecule in regulating plasminogen-mediated extracellular proteolysis is the urokinase-type plasminogen activator (uPA). To investigate the role of uPA in the invasive process of brain tumors, we stably transfected a human glioblastoma cell line SNB19 with a vector capable of expressing an antisense transcript complementary to the 1020 bases at the 3' end of the uPA cDNA. Parental, vector-, and antisense construct-stably transfected cell lines were analyzed for uPA mRNA transcript by Northern blot analysis, for uPA enzyme activity by zymography, and for uPA protein levels by Western blotting. The levels of uPA mRNA, protein, and enzyme activities were significantly lower in antisense clones than in parental and vector controls. Radioreceptor binding studies demonstrated that uPA receptor levels remained the same in parental, vector-, and antisense-transfected cells. The antisense-transfected cells showed a markedly lower level of invasion in the Ma-

trigel invasion assays, and their spheroids failed to invade the fetal rat brain aggregates in the coculture system. Green fluorescent protein (GFP) expressing parental and antisense transfectants was generated for detection in mouse brain tissue without any posttreatment. Intracerebral injection of antisense stable transfectants significantly reduced tumor formation compared with that in controls. Our results suggested that down-regulation of uPA expression may be a feasible approach to reducing the malignancy and invasiveness of glial tumors.

INTRODUCTION

The invasive ability of malignant cells depends on the concerted action of various cell surface-associated and -secreted proteases that promote the dissolution of surrounding matrix and basement membrane. A large body of evidence assigns a key role in tumor progression and invasion to uPA³ by virtue of its ability to initiate a cascade of proteases that can degrade most matrix and basement membrane components and interfere with cell-cell and cell-matrix interactions (1, 2). Bound to its cell surface receptor uPAR, uPA is the principal participant in ECM degradation (3, 4), as shown by the several-fold increase in plasminogen activation when uPA was bound to uPAR (4). Degradation of ECM has been shown to permit the release of such ECM-bound growth factors as epidermal and fibroblast growth factor, which participate in the regulation of cell proliferation (5). Moreover, the effect of uPA could depend on its ability to activate growth factors such as basic fibroblast growth factor (6), latent transforming growth factor- β (7), and pro-hepatocyte growth factor (8). Absence of uPA negatively affected the progression of chemically induced neoplasms in mice (9). Furthermore, the inoculation of metastatic Lewis lung carcinoma cells into plasminogen-deficient mice resulted in the formation of smaller and less hemorrhagic tumors than those observed in control wild-type mice (10). In addition to its proteolytic activity, uPA also has signal transduction properties, which can lead to changes in adhesive, mitogenic, and chemotactic responses of various cell types (11). A recent study found the mitogenic response to depend on both uPA activity and interaction with uPAR (12). However, in certain cell types some of the effects of uPA are independent of its proteolytic activity and uPAR binding (13, 14).

Malignant gliomas are characterized by rapid cell prolifer-

Received 8/11/00; revised 4/6/01; accepted 5/3/01.

The costs of publication of this article were defrayed in part by the payment of page charges. This article must therefore be hereby marked *advertisement* in accordance with 18 U.S.C. Section 1734 solely to indicate this fact.

¹ Supported by National Cancer Institute Grants CA 75557 (to J. S. R.) and P30 CA-16672. This work was completed at the University of Texas M. D. Anderson Cancer Center, Houston, TX.

² To whom requests for reprints should be addressed, at the Division of Cancer Biology, Department of Biomedical and Therapeutic Sciences, University of Illinois College of Medicine at Peoria, One Illini Drive, Box 1649, Peoria, IL 61656-1649. Phone: (309) 671-3445; Fax: (713) 671-3442; E-mail: jsrao@uic.edu.

³ The abbreviations used are: uPA, urokinase-type plasminogen activator; uPAR, uPA receptor; rPro-uPA, recombinant Pro-uPA; ECM, extracellular matrix; GAPDH, glyceraldehyde-3-phosphate dehydrogenase; GFP, green fluorescent protein; DiO, 3,3'-dioctadecyloxycarbocyanine perchlorate; Dil, 1,1 dioctadecyl-3,3,3',3'-tetramethylindocarbocyanine perchlorate.

ation, a high level of invasiveness into the surrounding brain, and increased vascularity. Diffuse astrocytomas, and especially glioblastoma multiforme in humans, invade the brain preferentially along white matter fiber tracts (15, 16) in rapid infiltrative growth that prevents successful surgical resection. Because local invasiveness contributes to the failure of curative treatment of glioblastoma, understanding the mechanisms of tumor invasiveness in the brain is central to controlling this disease. Dissolution of the ECM, a critical step in the process of invasion, requires proteolytic enzymes to promote hydrolysis of the surrounding ECM. Glioma cells mainly express components of the plasminogen activator system (17) and their expression of uPA was found to be much higher than that of adjacent non-neoplastic brain tissues (18–20). *In vivo* studies found that high levels of uPA correlated with shorter survival (21, 22). Several strategies, such as using antibodies against uPA and initiating tumor cell overexpression of recombinant mutant inactive uPA, have been used in the attempt to inhibit tumor invasiveness by blocking uPA-mediated generation of plasmin on tumor cell surfaces (23–26). Here, we report the direct blocking of uPA expression by the antisense approach in the human glioblastoma cell line SNB19. Our results support the concept that down-regulation of uPA expression by an antisense uPA vector may be important in decreasing the invasiveness of human gliomas.

MATERIALS AND METHODS

Cell Culture. Glioblastoma cells SNB19 were maintained in DMEM supplemented with 10% FCS at 37°C in a humidified CO₂ incubator and subcultured every 3–5 days.

Preparation of Constructs. A 1020-bp *Pst*I and *Eco*RI digest cDNA fragment of uPA (27) was blunt-ended and cloned in antisense orientation in a *Hind*III cut p β APr-1-neo (28) eukaryotic expression vector. The orientation and sequence of the insert was confirmed by automated sequencing, and analysis of the fragments generated by different restriction enzyme digestion.

Transfection of SNB19 Cells. The SNB19 cells were transfected with antisense uPA cDNA containing vector or empty vector, using lipofectin (Life Technologies, Inc., Gaithersburg, MD) as described earlier (29). Stable transfectants were selected with cloning cylinders after 3–4 weeks in medium containing G418 (800 μ g/ml). Cells transfected with expression vector alone served as controls. To identify individual tumor cells *in vivo* and to establish a way to monitor tumor cell migration during tumor formation, we transfected parental SNB19 cells and uPA antisense stable transfectants with the expression vector pEGFP-N1 (Clontech Laboratories, Palo Alto, CA). To obtain cells with high-level GFP expression, cells were plated in limiting dilution and bright green fluorescent colonies were visually selected, lifted, expanded, and subcloned by serial dilution to ensure purity.

Northern Blot Analysis. Total cellular RNA was extracted from confluent cultures as described earlier (29). Aliquots of 10 μ g of RNA were separated by electrophoresis on 1% agarose formaldehyde gel, capillary-transferred to a nylon membrane overnight, and cross-linked with UV irradiation. The filters were hybridized at 65°C with ³²P-radiolabeled uPA cDNA probe. Then the blots were stripped and rehybridized

with GAPDH to check loading equalities in transfer, and the results were normalized to GAPDH mRNA levels.

Zymography. Zymography was performed to determine the molecular size of plasminogen activators and their activities using the method described earlier (29). The samples were subjected to SDS-PAGE using 10% gels containing fibrinogen and plasminogen. The gel was then washed twice with 2.5% Triton X-100 for 30 min each time and incubated at 37°C overnight with 0.1 M glycine buffer (pH 7.5). The gel was stained with amido black and destained in a solution of 10% acetic acid and 50% methanol.

Western Blot Analysis. Serum-free culture supernatants were concentrated and applied on 10% polyacrylamide gels prepared as described earlier (29). Separated proteins were electroblotted onto a nitrocellulose membrane, and nonspecific binding was blocked by incubation with 5% milk powder in washing buffer. After being washed, the membrane was incubated with monoclonal antibodies against human uPA (Oncogene Research Products, Boston, MA), and protein was localized by the enhanced chemiluminescence-Western blotting detection system (Amersham Pharmacia Biotech, Piscataway, NJ).

Radioreceptor Assay. rPro-uPA was labeled with ¹²⁵I-iodide using Iodogen (Pierce, Rockford, IL), as described earlier (30). The cells were treated with acid buffer (pH 3.0) at room temperature for 3 min, washed four times and incubated with binding buffer consisting of DMEM, 0.1% BSA, and 20 mM HEPES with 4 nM radiolabeled rPro-uPA for 3 h at 4°C with and without a 50-fold excess of unlabeled rPro-uPA. At the end of the incubations, cells were washed four times, solubilized, and cell-bound radioactivity was counted in a gamma counter. Specific receptor binding was calculated as described previously (30).

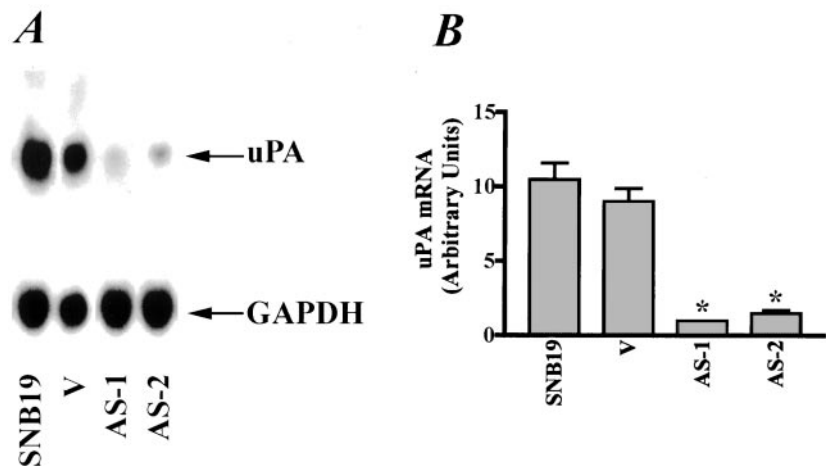
Matrigel Invasion Assay. Invasion of glioma cells *in vitro* was measured by the invasion of cells through Matrigel-coated transwell inserts. Briefly, transwell inserts with an 8- μ m pore size were coated with a final concentration of 1 mg/ml of Matrigel, cells were trypsinized, and 200 μ l of cell suspension (1 \times 10⁶ cells/ml) were added in triplicate wells. After 24 h incubation, cells that passed through the filter into the lower wells were quantitated as described earlier (29) and expressed as a percentage of the sum of cells in the upper and lower wells. Cells on the lower side of the membrane were fixed, stained with Hema-3, and photographed.

Glioma Spheroids. Multicellular glioma spheroids were cultured in 35 mm Petri dishes base-coated with 0.75% Noble agar prepared in DMEM. Briefly, 3 \times 10⁶ cells were suspended in 10 ml of medium, seeded onto 0.75% agar plates, and cultured until spheroids formed. Tumor spheroids were stained with fluorescent dye Dil and confronted with fetal rat brain aggregates that were stained with DiO (31).

Fetal Rat Brain Aggregates. Fetal rat brain aggregates were obtained from 18-day-old fetuses of Sprague Dawley rats. The brains were aseptically removed, minced, and dissociated by serial trypsinization. Single-cell suspension was obtained and plated into agar-coated multiwell plates. After 48 h, aggregates were transferred to new plates and cultured for 16 days.

Confocal Laser Scanning Microscopy. Invasion of the tumor spheroids into fetal rat brain aggregates was analyzed by confocal laser scanning microscopy (32). Briefly, Dil-stained

Fig. 1 **A**, Northern blot analysis of uPA mRNA in SNB19 and transfected cells. Total RNA was isolated, and 10 μ g of RNA was electrophoresed in 1% agarose gel and blotted onto a nylon membrane. The membrane was hybridized with 32 P-labeled uPA cDNA. After removal of the radiolabeled probe, the membrane was rehybridized with a GAPDH cDNA probe to check the relative amounts of mRNA loaded onto the gel. **B**, levels of uPA mRNA quantitated by scanning autoradiogram with laser densitometry. Relative hybridization signal numbers were calculated by ascribing an arbitrary value of 1 to the least intense signal seen by Northern blot analysis after loading equalities were determined based on the GAPDH probe. Data were shown as mean values \pm SD of four different experiments from each sample (*, $P < 0.001$).



tumor spheroids and DiO-stained fetal rat-brain aggregates were washed in the medium and transferred in quadruplicate to individual wells of a 96-well plate base-coated with agar. With the help of a sterile syringe and a stereomicroscope, tumor spheroids and fetal rat-brain aggregates were placed in close contact. At different time intervals, serial 1- μ m-thick optical sections were obtained from the surface to the center of the cocultures by a confocal laser scanning microscope. Dil and DiO fluorescence was detected by using an argon laser at 488 nm with a band-pass filter at 520–560 nm and a helium/neon laser at 543 nm with a long-pass filter at 590 nm, respectively. The remaining volume of the brain aggregate or tumor spheroid during cocultures at 24, 48, and 72 h was quantitated using the following formula: volume of aggregate = $(V1 + V2 + V3 + Vm) \times 2$.

Intracerebral Injection. Parental, vector-, and uPA antisense-transfected SNB19 cells were trypsinized and resuspended in serum-free medium. Mice were anesthetized, and 10- μ l aliquots of the cell suspension containing 2×10^6 cells in serum-free medium were injected using a stereotactic frame as described earlier (33). Eight animals were used for each group.

Tissue Preparation and Histochemical Staining. The mice were anesthetized and killed at 4 weeks postinjection by intracardiac perfusion with PBS, and then 4% paraformaldehyde in saline was used for *in situ* fixation of the tumor. The brains were removed, placed in 4% paraformaldehyde, and allowed to stand at 4°C. After 4 h, the brains were transferred to a solution of 0.5 M sucrose in PBS and incubated overnight at 4°C. The next day, the brain was cut and embedded in microscopic slides and frozen by placing at -20°C . Cryostat sections were stained with H&E to examine the tumor growth (33). The 10–12 sections were blindly reviewed and scored semiquantitatively for the size of the tumor in each case. The average cross sectional diameter measured in sections of each tumor was used to calculate tumor size and compared between controls and antisense transfectants. The variation between the sections in each group was <10%. Fluorescence microscopy was performed on tumor sections from GFP-expressing cells without any chemical treatment.

RESULTS

Isolation of uPA Antisense Construct Stably Transfected Clones. Human glioblastoma SNB19 cells were transfected with the empty ph β APr-1-neo vector and vector-containing uPA antisense construct. Vector-alone and uPA antisense construct-transfected cell lines were treated identically with regard to transfection conditions and maintenance in selection medium. Transfected cell lines were selected in the presence of G418 that had stably integrated the neoresistant gene-containing vector. Clones with empty vector and uPA antisense integrated construct were selected and analyzed for uPA expression and invasive capabilities in *in vitro* and *in vivo* assays.

Northern Blot Analysis of uPAR mRNA Levels Among Transfected Glioblastoma Clones. To determine whether the antisense constructs reduced uPA expression, we characterized SNB19 and its G418-resistant clones by Northern blot analysis and compared them with RNA from the parental cell line. Cell lines transfected with antisense vector showed substantially reduced mRNA encoding for uPA in all clones compared with those of parental cells and vector-alone-transfected clones (Fig. 1A). Quantitative uPA hybridization signals were determined after normalization with the GAPDH signal by densitometric scanning of the autoradiograms. Fig. 1B shows that uPA mRNA levels in antisense clones were decreased by ~8–10-fold compared with parental and vector clones ($P < 0.001$).

Measurement of uPA by Fibrin Zymography. To learn whether the antisense constructs reduced uPA secretion and its activity, we subjected the conditioned media from the transfected clones and parental cells to fibrin zymography. Fig. 2A shows that similar levels of uPA were present in the media of parental and vector-alone-transfected clones, but that uPA activity was reduced much less in uPA antisense clones. Quantitative enzymatic activity of uPA by densitometric scanning of the zymograms showed a significant ($P < 0.001$) by decrease of enzymatic activity (10–12-fold) in antisense clones compared with parental and vector clones (Fig. 2B).

Western Blot Analysis. To quantitate further the uPA protein content, the serum-free media of transfected and parental

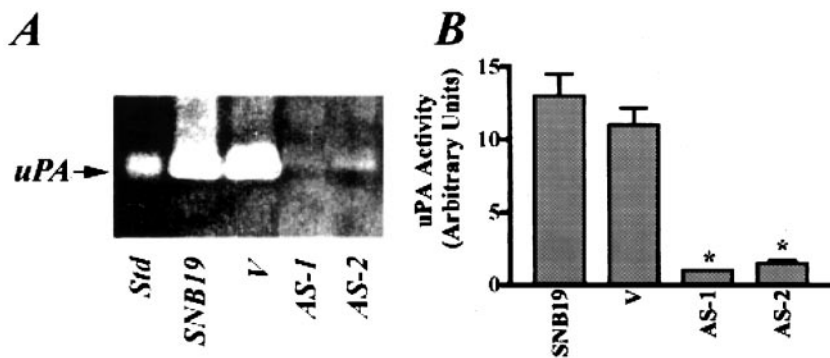
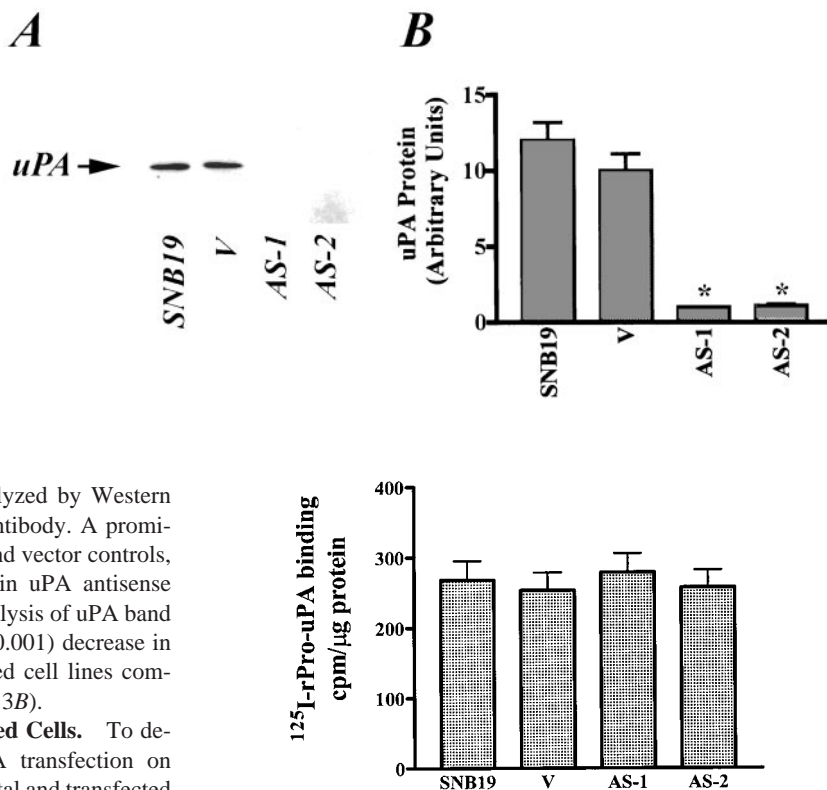


Fig. 2 A, fibrin zymography of medium from SNB19 and various clones. Conditioned medium (20 µg of protein) was run on 10% SDS-PAGE containing plasminogen and fibrinogen, as described in "Materials and Methods." B, uPA enzymatic activity was quantitated by scanning zymograms with laser densitometry. Data were shown as mean values of four different experiments from each sample (*, $P < 0.001$).

Fig. 3 A, immunoblot analysis of uPA in serum-free media of parental and uPA antisense-transfected human glioblastoma SNB19 cells using monoclonal antibodies, as described in "Materials and Methods." B, quantitative values of uPA protein were obtained by scanning the blot in three positions at different exposures and the peak areas were averaged. Data were shown as mean values ± SD of three different experiments from each clone (*, $P < 0.001$).



cells were subjected to SDS-PAGE and analyzed by Western blotting for uPA protein using monoclonal antibody. A prominent uPA band was present only in parental and vector controls, but was a very faint or undetectable band in uPA antisense stable transfectants (Fig. 3A). Quantitative analysis of uPA band by densitometry revealed a significant ($P < 0.001$) decrease in the uPA protein levels in antisense-transfected cell lines compared with parental and vector controls (Fig. 3B).

uPA Binding to SNB19 and Transfected Cells. To determine the effect of antisense uPA cDNA transfection on uPAR, we performed binding studies on parental and transfected cells using 125 I-labeled rPro-uPA. We found no marked difference in uPA binding sites between parental, vector-, and antisense-transfected clones (Fig. 4).

Invasive Potential Among Transfected Clones. To determine the effect of uPA antisense transfection, antisense transfectant clones were compared with parent SNB19 cells and vector transfectant in an *in vitro* Matrigel invasion assay. We found no marked difference in invasion between parental and vector-alone transfected clones, but we noted a significant inhibition of invasive potential with antisense transfected clones by staining (Fig. 5A). We found no marked difference in invasive potential that was noted between parental (42%) and vector (43%) but significantly ($P < 0.001$) reduced invasive potential in antisense clones (12%; Fig. 5B).

Inhibition of SNB19 Spheroid Invasion into Rat Brain Aggregates. To study the invasion of SNB19 cells in a more appropriate three-dimensional system, tumor spheroids and fetal

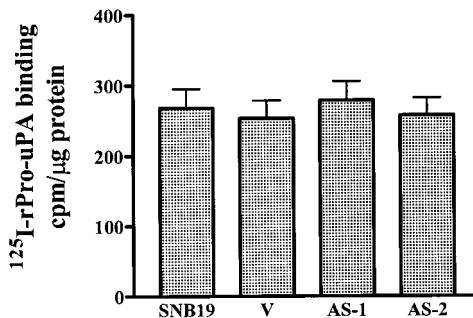


Fig. 4 rPro-uPA binding to SNB19 and transfected cell lines. Cells were pretreated with acid buffer and incubated at 4°C for 3 h with 4 nM 125 I-labeled rPro-uPA in the presence or absence of a 50-fold excess of unlabeled rPro-uPA. After incubation, cells were washed, lysed, and counted. Specific binding was determined as described in "Materials and Methods." Data were shown as mean values ± SD of four different experiments from each clone.

rat brain aggregates, which had been stained with fluorescent dyes Dil or DiO, were cocultured. Staining of the cells with these dyes allows better visualization and characterization of invasive pattern by confocal laser-scanning microscopy than do other *in vitro* invasion assays. When spheroids from parental, vector-, and uPA antisense construct-transfected clones were confronted with fetal rat brain aggregates, the coculture assays showed that vector-transfected and parental SNB19 cells pro-

Fig. 5 Invasion of human glioblastoma SNB19-, vector-, and antisense-transfected cells. A suspension of cells was layered on Matrigel-coated transwell clusters, and the percentage of invasion was calculated as described in "Materials and Methods." Cells invading through Matrigel-coated transwell inserts were stained (A) and the percentage of invading cells was quantified (B). Values are mean \pm SD of five different experiments from each clone (*, $P < 0.001$).

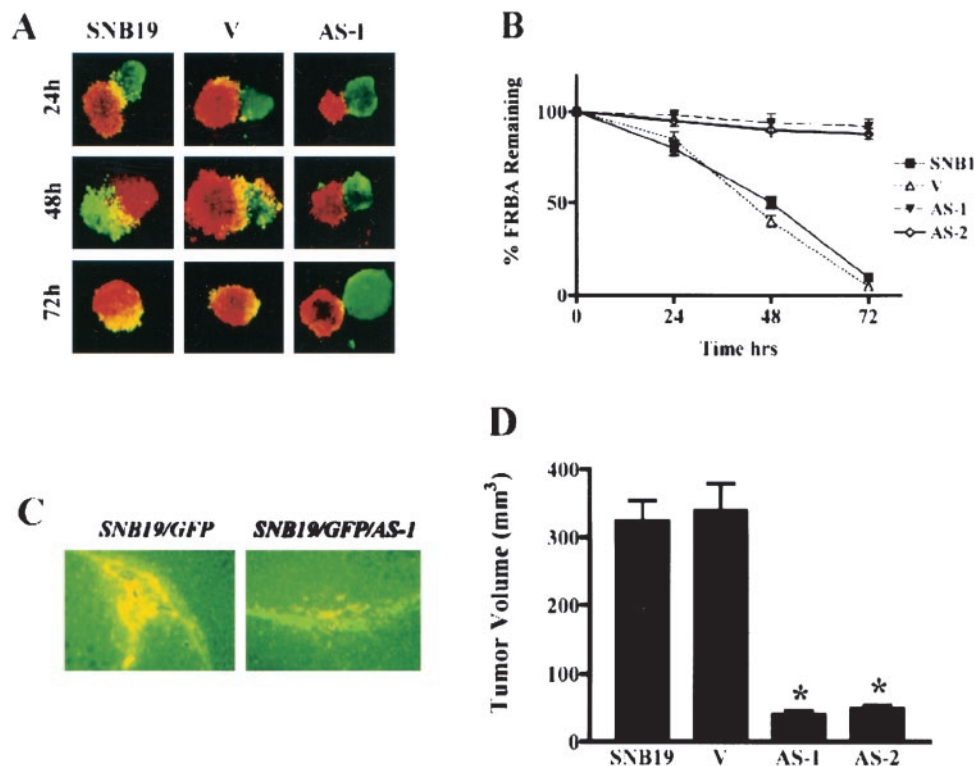
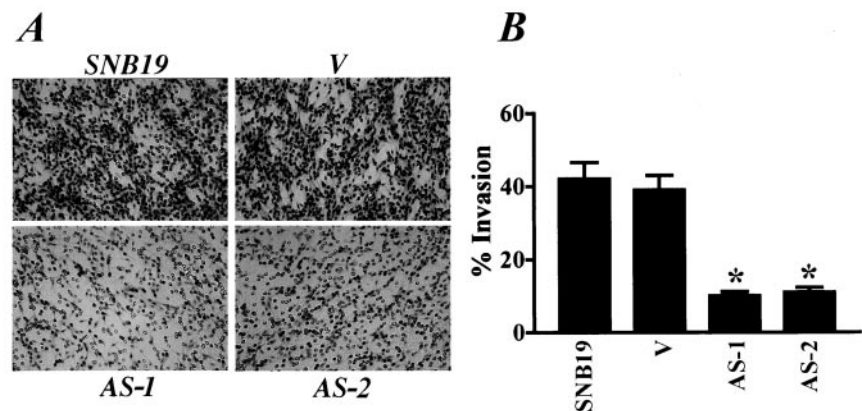


Fig. 6 A, confocal laser scanning images of SNB19 spheroids and rat brain aggregate cocultures scanned by laser scanning microscope at a depth of 100 μ m from the surface at different time intervals. The images represent the rat brain aggregates (green fluorescence) and parental-, vector-, or antisense-transfected tumor cell spheroids (red fluorescence). B, quantitation of remaining fetal rat brain aggregates by tumor spheroids as described in "Materials and Methods." Data shown are the mean \pm SD values from four separate experiments for each group. C, tumor formation by SNB19- and antisense-transfected cells in nude mouse brain. Photomicrograph of tumor sections from GFP-expressing cells (C) demonstrates lower GFP expression in tumor tissues derived from mouse brain injected with uPA antisense-transfected cells than in mouse brain injected with SNB19 glioblastoma cells. D, semiquantitation of tumor volume in parental, vector, and antisense clones 4 weeks after intracranial injection of these cells, as described in "Materials and Methods." Data shown are the \pm SD values from eight animals from each group (*, $P < 0.001$).

gressively invaded rat brain aggregates, causing a continuous decrease in the rat brain aggregate volume. In contrast, uPA antisense-transfected clones failed to invade rat brain aggregates (Fig. 6A). Quantitative analysis of the remaining fetal brain aggregates were 10–15% in parental and vector clones compared with 85–90% in antisense clones (Fig. 6B). The invasiveness of fetal rat brain aggregates was significantly decreased in

antisense clones compared with parental and vector-transfected clones ($P < 0.001$).

Tumor Formation in Nude Mice. To examine further the importance of reducing uPA levels, parental SNB19 cells and antisense uPA-transfected cells were injected intracerebrally into athymic mice. Each mouse injected with parental and vector-alone-transfected cells developed tumors. Histological

examination showed all tumors to behave in the infiltrative manner characteristic of gliomas. In contrast to mice that developed tumors when injected with parental SNB19 cells, mice injected with uPA antisense-transfected cells showed less tumor formation at 4 weeks postinjection. To visualize tumor cells *in vivo* without histological treatment of tissue, we injected parental and uPA antisense clones expressing GFP into nude mice brain. A marked reduction in tumor formation by uPA antisense clones was observed (Fig. 6C), demonstrating a reduction in invasiveness and tumor formation by antisense uPA in glioblastoma cells. These results showed that the tumorigenicity and *in vivo* growth of human glioblastoma are substantially inhibited by antisense uPA expression. The sections analyzed using H&E staining revealed that there was no significant difference in tumor size in mice that received an injection of parental and vector-transfected clone however, the tumor size was significantly reduced ($P < 0.001$) in antisense clones compared with parental and vector clones (Fig. 6D).

DISCUSSION

Tumor cell invasion is a complex, multistep process that is believed to involve the localized degradation of ECM, a crucial step in the invasion of surrounding tissue by tumor cells. A major protease system involved in tumor cell invasion is the plasminogen/plasmin system. The role of uPA, and particularly cell-surface uPA, as an initiator of ECM degradation and cellular invasiveness has been well established by *in vitro* and *in vivo* studies (1). uPA binding can transform uPAR from a simple receptor for uPA into a pleiotropic ligand (34) for other surface molecules. uPA is involved in the generation of plasmin, the activation of procollagenases and proforms of growth factors, and increased invasive and metastatic activity in various tumors (1, 35). Independent of its proteolytic activity, uPA is involved in the adhesion and motility of cells and signal transduction pathways, and its levels and activities are always found increased in malignant tumors (35).

Glioblastomas, the most common primary intracranial tumors, are extremely anaplastic and hypercellular with extensive nuclear polymorphism, and they are characterized by rapid cell proliferation, a high level of invasiveness into surrounding brain, and increased vascularity. Diffuse single-cell invasion, which occurs in all glial tumors regardless of histological grade, is defined as a translocation of neoplastic cells through host cellular and ECM barriers. Malignant gliomas have been shown to express greater quantities of uPA mRNA; in human gliomas, the level of expression seems to correlate with features of malignancy (36). Anti-uPA antibodies and uPA inhibitors have been shown to inhibit the invasiveness of tumor cells into ECM layers as well as amniotic and chick chorioallantoic membranes (37–39). Moreover, uPA antibodies blocked metastasis of Hep3 human carcinoma cells in chick embryos and inhibited the local invasiveness of Hep3 s.c. tumors in nude mice (23). Inhibition of uPA expression is, therefore, an attractive approach to blocking cellular invasiveness in cancer: down-regulation of uPA could reduce uPA-mediated proteolysis and various signaling pathways.

Strategies such as antisense inhibition of uPA have been used to inhibit the endogenous expression of uPA. In fibrin

matrix degradation assays, stable transfection of an expression plasmid pRc-RSV containing a uPA cDNA fragment of 647 bp in antisense orientation significantly reduced the invasiveness of the human ovarian cancer cell line OV-MZ-6 (40). The i.p. spread of human ovarian cancer cells in nude mice was significantly lower than that of control mice when the animals were treated with uPA antisense phosphorothioate oligonucleotides (41). An earlier report demonstrated that use of a 1020-bp 3' fragment of the uPA antisense cDNA was more effective in reducing uPA mRNA in an osteosarcoma cell line than was the entire uPA coding region or a 5' fragment (27). In the current study, we stably transfected glioblastoma cell line SNB19 with expression vectors containing a 1020-bp 3' portion of uPA cDNA in antisense orientation. Clones selected on the basis of their resistance to G418 were analyzed for uPA mRNA expression and enzyme activity. Stable antisense expression has been demonstrated to reduce endogenous uPA mRNA levels more effectively than parental and vector transfected clones. As an earlier study showed, treatment of a human T98G human glioblastoma cell line with uPA antisense phosphorothioate oligonucleotide resulted in greater decreases of uPA mRNA expression than did sense controls (42). The mechanisms involved in antisense inhibition are not fully known. They may include the blockage of gene expression, interference with RNA splicing, the inhibition of mRNA translation, and the induction of RNase III to cleave the double-stranded RNA after binding to target RNA. In our study, the secretion of uPA was markedly reduced in antisense clones compared with controls; however, the number of uPARs on the tumor cell surface was not affected by uPA antisense transfection.

Antisense-transfected clones showed a marked reduction in invasiveness in the Matrigel invasion assays over that of controls, suggesting that the modulation of uPA in SNB19 cells altered their invasive potential in the experimental model system. These findings are consistent with earlier reports concerning uPA antisense stable transfection in human ovarian cancer cell line OV-MZ-6 and antisense oligonucleotides in human esophageal carcinoma cell lines OC1 and OC3 (43). Haeckel *et al.* (27) showed, in Matrigel invasion assays, that transfecting human osteosarcoma cell line MNNG/HOS with antisense uPA vector suppressed its invasive ability. Our results of the Matrigel assay support the idea that uPA activity is crucial for invasion through Matrigel that contains a mixture of basement membrane components.

Spheroids, in which the malignant cells are organized in a three-dimensional network displaying cell-to-cell and cell-to-matrix contacts, represent an *in vitro* model for studies of the biology of malignant cells. One advantage of the spheroid model is that parallel behavior may be observed *in vivo* and *in vitro*. To know whether antisense transfected cells have similar invasive capabilities in coculture systems, we used a spheroid invasion assay to measure the ability of cells to invade fetal rat brain aggregates, and we found that the invasion of cells from tumor spheroids of antisense transfected clones was reduced compared with that of controls.

Because glioblastoma expresses high levels of uPA during invasion and its expression correlates with tumor progression, we reasoned that efficient reduction of uPA could possibly inhibit the growth of tumors in nude mice. Indeed, our results

demonstrated that cells expressing antisense cDNA for uPA formed significantly smaller tumors in the brains of nude mice compared with the parental SNB19 cells, whose characteristic invasive behavior resulted in progressive tumor growth. These observations consolidate the notion that cells overexpressing uPA are more invasive in normal brain. In an earlier study in which a chorioallantoic membrane assay was used, stable transfection of human osteosarcoma cell line MNNG/HOS with antisense uPA vector was shown to suppress the ability of the cells to metastasize (27).

Antisense therapy for cancer has potential effectiveness as an alternative to conventional cancer therapy. The viable established stable cell line provides a good model for characterizing phenotypic changes associated with suppressed endogenous uPA expression. Whatever the underlying mechanism may be, inhibition of uPA gene expression tends to reverse the invasiveness and tumor formation characteristics of glioblastoma cells, and it appears to be a promising adjuvant approach to the treatment of disseminated glioblastoma.

ACKNOWLEDGMENTS

We thank Lydia Soto for preparing the manuscript and Lore Feldman for manuscript review.

REFERENCES

- Andreasen, P. A., Kjoller, L., Christensen, L., and Duffy, M. J. The urokinase-type plasminogen activator system in cancer metastasis: a review. *Int. J. Cancer*, *72*: 1–22, 1997.
- Carrroll, V. A., and Binder, B. R. The role of the plasminogen activation system in cancer. *Semin. Thromb. Hemost.*, *25*: 183–197, 1999.
- Alonso, D. F., Farias, E. F., Ladeda, V., Davel, L., Puricelli, L., and Bal de Kier Joffe, E. Effects of synthetic urokinase inhibitors on local invasion and metastasis in a murine mammary tumor model. *Breast Cancer Res. Treat.*, *40*: 209–223, 1996.
- Ellis, V., Behrendt, N., and Dano, K. Plasminogen activation by receptor-bound urokinase. A kinetic study with both cell-associated and isolated receptor. *J. Biol. Chem.*, *266*: 12752–12758, 1991.
- Werb, Z., Ashkenas, J., MacAuley, A., and Wiesen, J. F. Extracellular matrix remodeling as a regulator of stromal-epithelial interactions during mammary gland development, involution and carcinogenesis. *Braz. J. Med. Biol. Res.*, *29*: 1087–1097, 1996.
- Odekon, L. E., Sato, Y., and Rifkin, D. B. Urokinase-type plasminogen activator mediates basic fibroblast growth factor-induced bovine endothelial cell migration independent of its proteolytic activity. *J. Cell. Physiol.*, *150*: 258–263, 1992.
- Odekon, L. E., Blasi, F., and Rifkin, D. B. Requirement for receptor-bound urokinase in plasmin-dependent cellular conversion of latent TGF- β to TGF- β . *J. Cell. Physiol.*, *158*: 398–407, 1994.
- Naldini, L., Vigna, E., Bardelli, A., Follenzi, A., Galimi, F., and Comoglio, P. M. Biological activation of pro-HGF (hepatocyte growth factor) by urokinase is controlled by a stoichiometric reaction. *J. Biol. Chem.*, *270*: 603–611, 1995.
- Shapiro, R. L., Duquette, J. G., Roses, D. F., Nunes, I., Harris, M. N., Kamino, H., Wilson, E. L., and Rifkin, D. B. Induction of primary cutaneous melanocytic neoplasms in urokinase-type plasminogen activator (uPA)-deficient and wild-type mice: cellular blue nevi invade but do not progress to malignant melanoma in uPA-deficient animals. *Cancer Res.*, *56*: 3597–3604, 1996.
- Bugge, T. H., Kombrinck, K. W., Xiao, Q., Holmback, K., Daugherty, C. C., Witte, D. P., and Degen, J. L. Growth and dissemination of Lewis lung carcinoma in plasminogen-deficient mice. *Blood*, *90*: 4522–4531, 1997.
- Blasi, F. Proteolysis, cell adhesion, chemotaxis, and invasiveness are regulated by the u-PA-u-PAR-PAI-1 system. *Thromb. Haemost.*, *82*: 298–304, 1999.
- Stepanova, V., Mukhina, S., Kohler, E., Resink, T. J., Erne, P., and Tkachuk, V. A. Urokinase plasminogen activator induces human smooth muscle cell migration and proliferation via distinct receptor-dependent and proteolysis-dependent mechanisms. *Mol. Cell. Biochem.*, *195*: 199–206, 1999.
- Koopman, J. L., Slomp, J., de Bart, A. C., Quax, P. H., and Verheijen, J. H. Mitogenic effects of urokinase on melanoma cells are independent of high affinity binding to the urokinase receptor. *J. Biol. Chem.*, *273*: 33267–33272, 1998.
- Longstaff, C., Merton, R. E., Fabregas, P., and Felez, J. Characterization of cell-associated plasminogen activation catalyzed by urokinase-type plasminogen activator, but independent of urokinase receptor (uPAR, CD87). *Blood*, *93*: 3839–3846, 1999.
- Pedersen, P. H., Edvardsen, K., Garcia-Cabrera, I., Mahesparan, R., Thorsen, J., Mathisen, B., Rosenblum, M. L., and Bjerkvig, R. Migratory patterns of lac-z transfected human glioma cells in the rat brain. *Int. J. Cancer*, *62*: 767–771, 1995.
- Giese, A., and Westphal, M. Glioma invasion in the central nervous system. *Neurosurgery*, *39*: 235–250, 1996.
- MacDonald, T. J., DeClerck, Y. A., and Laug, W. E. Urokinase induces receptor mediated brain tumor cell migration and invasion. *J. Neurooncol.*, *40*: 215–226, 1998.
- Gladson, C. L., Pijuan-Thompson, V., Olman, M. A., Gillespie, G. Y., and Yacoub, I. Z. Up-regulation of urokinase and urokinase receptor genes in malignant astrocytoma. *Am. J. Pathol.*, *146*: 1150–1160, 1995.
- Yamamoto, M., Sawaya, R., Mohanam, S., Bindal, A. K., Bruner, J. M., Oka, K., Rao, V. H., Tomonaga, M., Nicolson, G. L., and Rao, J. S. Expression and localization of urokinase-type plasminogen activator in human astrocytomas *in vivo*. *Cancer Res.*, *54*: 3656–3661, 1994.
- Sandstrom, M., Johansson, M., Sandstrom, J., Bergenheim, A. T., and Henriksson, R. Expression of the proteolytic factors, tPA and uPA, PAI-1 and VEGF during malignant glioma progression. *Int. J. Dev. Neurosci.*, *17*: 473–481, 1999.
- Bindal, A. K., Hammoud, M., Shi, W. M., Wu, S. Z., Sawaya, R., and Rao, J. S. Prognostic significance of proteolytic enzymes in human brain tumors. *J. Neuro-Oncol.*, *22*: 101–110, 1994.
- Hsu, D. W., Efid, J. T., and Hedley-Whyte, E. T. Prognostic role of urokinase-type plasminogen activator in human gliomas. *Am. J. Pathol.*, *147*: 114–123, 1995.
- Ossowski, L., Russo-Payne, H., and Wilson, E. L. Inhibition of urokinase-type plasminogen activator by antibodies: the effect on dissemination of a human tumor in the nude mouse. *Cancer Res.*, *51*: 274–281, 1991.
- Kobayashi, H., Gotoh, J., Shinohara, H., Moniwa, N., and Terao, T. Inhibition of the metastasis of Lewis lung carcinoma by antibody against urokinase-type plasminogen activator in the experimental and spontaneous metastasis model. *Thromb. Haemostasis*, *71*: 474–480, 1994.
- Crowley, C. W., Cohen, R. L., Lucas, B. K., Liu, G., Shuman, M. A., and Levinson, A. D. Prevention of metastasis by inhibition of the urokinase receptor. *Proc. Natl. Acad. Sci. USA*, *90*: 5021–5025, 1993.
- Evans, C. P., Elfman, F., Parangi, S., Conn, M., Cunha, G., and Shuman, M. A. Inhibition of prostate cancer neovascularization and growth by urokinase-plasminogen activator receptor blockade. *Cancer Res.*, *57*: 3594–3599, 1997.
- Haeckel, C., Krueger, S., and Roessner, A. Antisense inhibition of urokinase: effect on malignancy in a human osteosarcoma cell line. *Int. J. Cancer*, *77*: 153–160, 1998.
- Gunning, P., Leavitt, J., Muscat, G., Ng, S. Y., and Kedes, L. A human β -actin expression vector system directs high-level accumulation of antisense transcripts. *Proc. Natl. Acad. Sci. USA*, *84*: 4831–4835, 1987.
- Mohanam, S., Chintala, S. K., Go, Y., Bhattacharya, A., Venkaiah, B., Boyd, D., Gokaslan, Z. L., Sawaya, R., and Rao, J. S. *In vitro*

- inhibition of human glioblastoma cell line invasiveness by antisense uPA receptor. *Oncogene*, *14*: 1351–1359, 1997.
30. Mohanam, S., Sawaya, R., McCutcheon, I., Ali-Osman, F., Boyd, D., and Rao, J. S. Modulation of *in vitro* invasion of human glioblastoma cells by urokinase-type plasminogen activator receptor antibody. *Cancer Res.*, *53*: 4143–4147, 1993.
31. Pedersen, P. H., Marienhagen, K., Mork, S., and Bjerkvig, R. Migratory pattern of fetal rat brain cells and human glioma cells in the adult rat brain. *Cancer Res.*, *53*: 5158–5165, 1993.
32. Nygaard, S. J., Pedersen, P. H., Mikkelsen, T., Terzis, A. J., Tysnes, O. B., and Bjerkvig, R. Glioma cell invasion visualized by scanning confocal laser microscopy in an *in vitro* co-culture system. *Invasion Metastasis*, *15*: 179–188, 1995.
33. Go, Y., Chintala, S. K., Oka, K., Gokaslan, Z., Sawaya, R., and Rao, J. S. Invasive pattern of lac-Z-transfected human glioblastoma cells in nude mice brain. *Cancer Lett.*, *110*: 225–231, 1996.
34. Dear, A. E., and Medcalf, R. L. The urokinase-type-plasminogen-activator receptor (CD87) is a pleiotropic molecule. *Eur. J. Biochem.*, *252*: 185–193, 1998.
35. Schmitt, M., Harbeck, N., Thomssen, C., Wilhelm, O., Magdolen, V., Reuning, U., Ulm, K., Hofler, H., Janicke, F., and Graeff, H. Clinical impact of the plasminogen activation system in tumor invasion and metastasis: prognostic relevance and target for therapy. *Thromb. Haemost.*, *78*: 285–296, 1997.
36. Arai, Y., Kubota, T., Nakagawa, T., Kabuto, M., Sato, K., and Kobayashi, H. Production of urokinase-type plasminogen activator (u-PA) and plasminogen activator inhibitor-1 (PAI-1) in human brain tumours. *Acta Neurochir. (Wien.)*, *140*: 377–385, 1998.
37. Holst-Hansen, C., Johannessen, B., Hoyer-Hansen, G., Romer, J., Ellis, V., and Brunner, N. Urokinase-type plasminogen activation in three human breast cancer cell lines correlates with their *in vitro* invasiveness. *Clin. Exp. Metastasis*, *14*: 297–307, 1996.
38. Jarrard, D. F., Hansen, N. M., Patai, B., and Rukstalis, D. B. Urokinase plasminogen activator is necessary but not sufficient for prostate cancer cell invasion. *Invasion Metastasis*, *15*: 34–45, 1995.
39. Alonso, D. F., Tejera, A. M., Farias, E. F., Bal de Kier Joffe, E., and Gomez, D. E. Inhibition of mammary tumor cell adhesion, migration, and invasion by the selective synthetic urokinase inhibitor B428. *Anti-cancer Res.*, *18*: 4499–4504, 1998.
40. Fischer, K., Lutz, V., Wilhelm, O., Schmitt, M., Graeff, H., Heiss, P., Nishiguchi, T., Harbeck, N., Kessler, H., Luther, T., Magdolen, V., and Reuning, U. Urokinase induces proliferation of human ovarian cancer cells: characterization of structural elements required for growth factor function. *FEBS Lett.*, *438*: 101–105, 1998.
41. Wilhelm, O., Schmitt, M., Hohl, S., Senekowitsch, R., and Graeff, H. Antisense inhibition of urokinase reduces spread of human ovarian cancer in mice. *Clin. Exp. Metastasis*, *13*: 296–302, 1995.
42. Engelhard, H., Narang, C., Homer, R., and Duncan, H. Urokinase antisense oligodeoxynucleotides as a novel therapeutic agent for malignant glioma: *in vitro* and *in vivo* studies of uptake, effects and toxicity. *Biochem. Biophys. Res. Commun.*, *227*: 400–405, 1996.
43. Morrissey, D., O'Connell, J., Lynch, D., O'Sullivan, G. C., Shanahan, F., and Collins, J. K. Invasion by esophageal cancer cells: functional contribution of the urokinase plasminogen activation system, and inhibition by antisense oligonucleotides to urokinase or urokinase receptor. *Clin. Exp. Metastasis*, *17*: 77–85, 1999.